



## Investigation of the particle growth of fenofibrate following antisolvent precipitation and freeze-drying

Teresa B. Tierney, Yina Guo, SERGEY BELOSHAPKIN, AKE RASMUSON, SARAH HUDSON

### Publication date

01-01-2015

### Published in

Crystal Growth and Design;15 (1), pp. 5213-5222

### Licence

This work is made available under the [CC BY-NC-SA 1.0](#) licence and should only be used in accordance with that licence. For more information on the specific terms, consult the repository record for this item.

### Document Version

1

### Citation for this work (HarvardUL)

Tierney, T.B., Guo, Y., BELOSHAPKIN, S., RASMUSON, A. and HUDSON, S. (2015) 'Investigation of the particle growth of fenofibrate following antisolvent precipitation and freeze-drying', available: <https://hdl.handle.net/10344/5351> [accessed 24 Aug 2022].

This work was downloaded from the University of Limerick research repository.

For more information on this work, the University of Limerick research repository or to report an issue, you can contact the repository administrators at [ir@ul.ie](mailto:ir@ul.ie). If you feel that this work breaches copyright, please provide details and we will remove access to the work immediately while we investigate your claim.

# An Investigation of the Particle Growth of Fenofibrate following Antisolvent Precipitation and Freeze-drying

*Teresa B. Tierney<sup>†\*</sup>, Yina Guo<sup>\*</sup>, Sergey Beloshapkin<sup>\*</sup>, Åke C. Rasmuson<sup>†\*</sup>, and Sarah P. Hudson<sup>†\*#</sup>*

<sup>†</sup> Synthesis and Solid State Pharmaceutical Centre, <sup>†</sup>Department of Chemical and Environmental Sciences, <sup>\*</sup>Materials and Surface Science Institute, University of Limerick, Limerick, Ireland.

**ABSTRACT:** Submicron to small-micron sized particles of the hydrophobic drug, fenofibrate, were prepared by controlled crystallisation in order to influence its dissolution behaviour. An antisolvent precipitation process successfully generated particles (200-300 nm) which matched the size and dissolution behaviour of a commercial wet-milled formulation of the drug. Although the preparation of submicron sized particles was straightforward, retaining their size in suspension and during isolation was a challenge. Additives were employed to temporarily stabilise the suspension, and extend the time window for isolation of the submicron particles. Precipitated particles were isolated primarily by immediate freeze-drying, but drying stresses were found to destabilise the fragile submicron system. The growth pathway of particles in suspension, and during oven and freeze-drying were compared. Although the growth pathways appeared considerably different from a visual morphological perspective, an investigation of the

electron diffraction patterns, and the inner-particle surfaces showed that the growth pathways were the same; molecular addition by Ostwald ripening. The observed differences in the time-resolved particle morphologies were found to be a result of the freeze-drying process.

## **1. INTRODUCTION**

It is estimated that 40% of new chemical entities fail to reach commercialization because of their poor water-solubility, dissolution rates and oral bioavailability, which combine to cause administration difficulties <sup>1</sup>. An orally administered drug must dissolve in the gastrointestinal (GI) tract before permeating through lipophilic physiological barriers and entering the blood stream. While a degree of lipophilicity aids transportation of the drug across these barriers, it can hinder its dissolution ability in the aqueous environment of the GI tract. Poor drug dissolution can lead to incomplete and irregular absorption. Consequently, the dose must be increased or administered with food to enhance the dissolution and achieve the necessary therapeutic requirements. One feasible strategy to alleviate food effects and improve the dissolution properties of water-insoluble (BCS Class II and IV) drugs is to decrease their particle size <sup>2</sup>. According to the Noyes Whitney equation, reducing the particle size and so increasing the specific surface area, leads to an increase in the dissolution rate <sup>3</sup>. Size reduction of poorly water-soluble drugs to the submicron scale offers the opportunity to address many of the deficiencies associated with hydrophobic drug formulations and could potentially save many prospective drug candidates from abandonment after discovery.

Examples of commercially available oral drug formulations which utilize submicron particles to reach their delivery goals include; RAPAMUNE (sirolimus, milled), EMEND (aprepitant, milled), TriCor (fenofibrate, milled), MEGACE ES (megestrol acetate, milled), and Triglide (fenofibrate, jet-stream homogenized) <sup>4</sup>. Currently, diminution techniques such as milling are the

most popular industrial approaches to generate submicron particles. However, these techniques are grossly energy intensive and inefficient, with only 1-2% of the applied energy being used for size reduction <sup>5</sup>. Diminution processes also limit control of particle size, morphology and surface properties, can take long times to achieve the required size, can introduce impurities from abrasion of the milling media, and can lead to thermal/mechanical degradation of temperature-sensitive materials <sup>6-8</sup>.

Controlled crystallization/precipitation offers a potentially more efficient approach to generate fine particles, with better control over the particle properties. Antisolvent precipitation could provide a cheap and technologically easy route to the industrial production of submicron particles by using a simple process at ambient conditions, and low cost equipment with good scale-up prospects. While industrial applications of the antisolvent process are so far limited, this approach to fine particle production has been used in many academic studies. Particle sizes of the hydrophobic drugs beclomethason dipropionate <sup>6</sup>, carbamazepine <sup>9</sup> and deflazocort <sup>10</sup> were manipulated by varying certain parameters of the antisolvent precipitation process when water was used as the antisolvent. However, in the preparation of submicron to small micron sized particles, additives are usually required to stabilize the precipitated particles against growth and aggregation <sup>11</sup>. Common pharmaceutical stabilizers include polymers: cellulose derivatives, povidones, phospholipids, poloxamers (pluronic); and surfactants: Tween-80 and sodium dodecyl sulphate (SDS). Khan et al. (2013) used additive-controlled antisolvent precipitation to stabilize suspended particles of artemisinin (400 nm), ibuprofen (92 nm) and glyburide (298 nm) for 30 days using combinations of Pluronic F127, PVP-K30, HPMC and sodium deoxycholate <sup>12</sup>. Hu et al. used a similar approach to temporarily stabilize a suspension of fenofibrate (300-400 nm) for 6 minutes using HPMC, SDS and lactose <sup>11</sup>.

Particles prepared by antisolvent precipitation can grow by the traditional mechanism of molecular addition (ie. Ostwald ripening) or by the more recently proposed oriented-attachment and assembly mechanism<sup>13, 14</sup>. Unlike traditional molecule-by-molecule crystal growth, growth by oriented attachment occurs through self-assembly of primary submicron particles into ordered superstructures or ‘mesocrystals’, which can subsequently fuse to form a single crystal<sup>13, 14</sup>.

In this work, submicron sized particles of a model drug, fenofibrate, were prepared using a simple antisolvent precipitation process. The submicron particles were stabilized in suspension using a series of additives, and a discussion is herein provided as to why the additives have superior or inferior stabilization capabilities based on the molecular chemistry of both the drug and the additive molecules. The novelty of the work lies not only in the improved stabilization achieved here compared to a previous report, under comparable conditions<sup>11</sup>, but also in the investigation into the effect of freeze-drying, and the effect of stabilizer presence during freeze-drying, on the final size, morphology and observed growth pathway, which has not been reported elsewhere. Here, we highlight the influence of the isolation process on the resulting size and morphology, and the corresponding influence of both the size and morphology on the dissolution rate. These isolation-related effects were found to be particularly critical when trying to obtain submicron particles in the solid form.

Fenofibrate (FF) is a cholesterol-controlling, BCS class II hydrophobic drug (log P 5.3) with extremely limited solubility in water (< 0.5 µg/mL at 25°C<sup>15</sup>). The drug in its conventional form has restricted oral bioavailability and exhibits positive food effects (absorption is 35% higher in fed state). Particle size reduction to the submicron range eliminates food requirements<sup>16</sup>. The molecular structure of FF is shown in Figure 1.

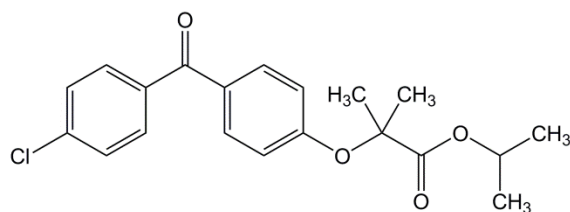


**Figure 1.** Molecular structure of fenofibrate.

## 2. EXPERIMENTAL SECTION

**2.1 Materials.** Fenofibrate (FF) (99.7% purity) was generously gifted from Abbvie Laboratories. Ethanol (99.8% purity) was purchased from Merck Millipore. Stabilizers; polyvinyl alcohols (PVA, MW: 9-10 kDa, 13-23 kDa, 85-124 kDa, 146-186 kDa), hydroxypropyl methyl cellulose (HPMC, ~ 26 kDa), sodium dodecyl sulphate (SDS), d-lactose monohydrate (lactose), polyvinyl pyrrolidone K30 (PVP-K30, 40 kDa), Pluronic F127 (~12.5 kDa) and Kolliphor 188 (7-9 kDa) were purchased from Sigma Aldrich and polyethylene glycol (PEG, 3.4 kDa) was purchased from Polysciences Inc.. Hydrochloric acid and Tween-80 were purchased from Sigma Aldrich for use in dissolution testing. TriCor tablets (commercial submicron formulation) were purchased from Abbott.

**2.2. Antisolvent process parameters.** The solubility of FF in ethanol at 25°C was gravimetrically determined. The antisolvent process conditions were optimized by monitoring the effects of drug concentration (10, 30, 50 mg/mL), antisolvent to solvent (AS/S) volume ratio (5, 10, 20, 40 [constant FF mass in AS/S mixture: 1.82 mg/mL]), agitation rate (200, 500, 800 rpm) and aging time (up to 31 min) on the resulting size and morphology after precipitation. The AS/S experimental set was conducted at 30°C. All other experiments were conducted at 25°C.

**2.3. Effect of additives on the antisolvent process.** An organic solution of FF in ethanol (1 mL, 50 mg/mL) was quickly introduced by eppendorf pipette to water (10 mL) with or without

additives at the compositions outlined in Table 1. Solutions/suspensions were maintained at a constant temperature of 25°C under rapid agitation (800 rpm) throughout the precipitation process. On contact with the antisolvent, the FF immediately precipitated giving a fine milky suspension. In cases where the particles were dried, the FF suspension was flash frozen in liquid nitrogen and freeze-dried under vacuum (< 27 Pa) for 48 h using a Dura-Dry Microprocessor Control freeze-dryer. Alternatively, a drop of suspension was quickly oven-dried at 55°C. The reference sample refers to an un-stabilized system in which no additives were present in the antisolvent during precipitation.

**Table 1.** Additive systems used during antisolvent precipitation

Expt.	Additive system	Additive conc. in AS (%w/v)
Additive screening	PVP-K30	0.1 %
	Pluronic F127	
	PVA	
	HPMC	
	SDS	
	Kolliphor 188	
	PEG	
	Combinations of above additives	0.1 % each
PVA: molecular weight	PVA (9-10 kDa)	0.1 %
	PVA (13-23 kDa)	
	PVA (85-124 kDa)	
	PVA (146-186 kDa)	
PVA: Conc.	PVA (9-10 kDa)	0.01 %
		0.05 %
		0.1 %
		0.2 %
		0.35 %
		0.5 %
		0.75 %
		2.0 %
Prep A	No additives (reference)	N/A
Prep B	HPMC	0.05 %

	SDS	0.05 %
	Lactose	1 %
Prep C	PVA (9-10 kDa)	0.2 %

**2.4. Particle size analysis.** Particle size measurements were performed by laser diffraction on a Malvern Mastersizer 2000, with water as the dispersion medium. Precipitated suspensions were diluted by a factor of 5 with water (0.91 mg/mL FF) prior to their introduction to the sample chamber. An obscuration of 7-10%, a stir rate of 2600 rpm, a one minute pre-measurement delay and 5% sonication power (wrt Malvern Mastersizer 2000 sonication scale) were used during all size measurements. Runs were conducted at room temperature and 4 measurements were recorded for each run. When no stabilizing additives were present during precipitation, HPMC and SDS were added to the water dispersant (0.038 mg/mL) to minimize variation between 4 consecutive measurements. Size distributions for FF were calculated using a refractive index of 1.55 and an absorption index of 0.01. Freeze-dried particles were redispersed in water at 0.91 mg/mL before size measurements. The D[4,3] volume-weighted mean diameter was reported for each size distribution. Sizing experiments were carried out at least in duplicate.

The size of FF particles in TriCor tablets were measured using dynamic light scattering on a Malvern Zetasizer. Tablets were ground with a pestle and mortar for 2 minutes and the powder was suspended in water (1 mg/mL FF). The large insoluble excipients were removed by vacuum filtration through a hydrophilic 1.2  $\mu\text{m}$  Millipore membrane filter (RAFT04700). The size of the sub-1.2  $\mu\text{m}$  particles was measured and these particles were captured by further filtering the suspension through a 0.22  $\mu\text{m}$  PVDF membrane filter. FTIR (Perkin Elmer Spectrum 100 FT-IR Spectrometer) confirmed that the submicron particles were FF.

**2.5. Scanning Electron Microscopy.** Sizes and morphologies of particles in dried samples were analyzed using a Hitachi SU-70 high-resolution scanning electron microscope (SEM).



Freeze-dried particles were placed directly on carbon tape on an aluminum stub. Oven-dried particles were prepared by drying the suspension directly on the carbon tape in an oven at 55°C (drying took approx. 12 min). For both preparation methods, samples were coated with an ~8 nm gold deposit using an EMITECH K55 and the particles were imaged in field-free mode at a voltage of 10 kV and a working distance of 10 mm. The image analysis software, ImageJ, was used to analyze particle sizes from SEM images. All SEM images show particles which were fully representative of the entire sample analyzed in each case.

**2.6. X-ray diffraction.** Powder X-ray diffraction (XRD) was used to identify the polymorphic form and to monitor the degree of crystallinity of the ‘as received’ and precipitated samples. Diffraction patterns were recorded using a PANalytical Empyrean diffractometer in transmission mode using Ni filtered Cu K $\alpha$  radiation ( $\lambda = 1.54 \text{ \AA}$ ) at 40 kV and 40 mA. Powder samples were prepared by trapping a small amount of powder between two strips of amorphous scotch tape and scanning the samples in the angular range of 5° (2 $\theta$ ) to 35° (2 $\theta$ ).

**2.7. Transmission Electron Microscopy and Electron Diffraction.** Surface morphology analysis and selected area electron diffraction (SAED) of freeze-dried PVA-precipitated FF particles were conducted using a transmission electron microscope (TEM, Joel JEM-2011 equipped with GATAN Multiscan CCD camera, model 794) at an accelerating voltage of 200 kV. The dried samples were suspended in deionized water and placed in a sonication bath for 30 min before applying a drop of the suspension to a holey carbon-supported TEM grid and air drying overnight. Diffraction patterns were obtained before TEM imaging to minimize the effects of beam damage on the diffraction results.

**2.8. Focused Ion Beam.** A focused ion beam (FIB) system (FEI 200, 30 kV, Ga<sup>+</sup> ions) was employed to cut through the precipitated FF particles. Particles were mounted on an aluminum

stub and gold-coated before analysis. The part of the particle to be protected from the beam was coated with a 1  $\mu\text{m}$  layer of platinum. The cut particles were tilted through  $45^\circ$  and their cross-sections were imaged. Three particles were analyzed for each sample studied.

**2.9. Dissolution studies.** A 0.1M HCl solution containing 0.4% w/v Tween-80 was used as the dissolution medium (DM).

*2.9.1. Solubility:* Prior to dissolution rate testing, the solubility of FF ('as received', TriCor and precipitated samples) in the DM was measured in order to determine sink conditions for dissolution testing. The solubility was determined by UV/vis spectroscopy (Cary 300 Bio,  $\lambda$  - 288 nm) by increasing the FF amount in the DM until the saturation limit was reached, as seen by a plateau effect in the calibration curve.

*2.9.2. Dissolution rate testing:* Dissolution tests were carried out in sink conditions at approx. 1/5 of the solubility concentration. Tests were carried out at  $42^\circ\text{C}$  and conducted by adding a sample (solid or suspension) containing 25 mg FF to 900 mL of the DM. TriCor tablets were ground by pestle and mortar for 2 min, prior to dissolution testing. After sample addition, 4 mL aliquots were taken at regular intervals from the bulk solution in preheated ( $45^\circ\text{C}$ ) plastic syringes and filtered through preheated ( $45^\circ\text{C}$ ) PTFE 0.2  $\mu\text{m}$  syringe filters. The dissolved FF concentration was measured by UV/visible spectroscopy (Cary 300 Bio,  $\lambda$  - 288 nm). Dissolution rates are expressed as the % dissolved/second over the first 30 seconds of dissolution. Dissolution tests were carried out at least in duplicate. It was noted that the presence of ethanol (0.055 mL/100 mL DM) in the suspended samples had no significant impact on the dissolution rate or overall solubility.

### 3. RESULTS

**3.1. Effect of antisolvent process parameters.** The solubility of FF in ethanol at 25°C was found to be 63 mg/mL. The highest drug concentration tested during antisolvent precipitation (Prep A, 50 mg/mL) produced the smallest particles (200-300 nm, aging time 0.5 min), with a monomodal distribution, Figure 2. Lower drug concentrations produced bimodal distributions consisting of both submicron and micron range particles. The antisolvent to solvent (AS/S) volume ratio and the agitation rate had no obvious impact on the particle size over the ranges tested (Figure S1).

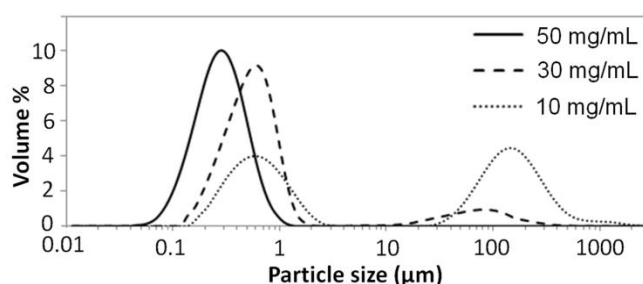


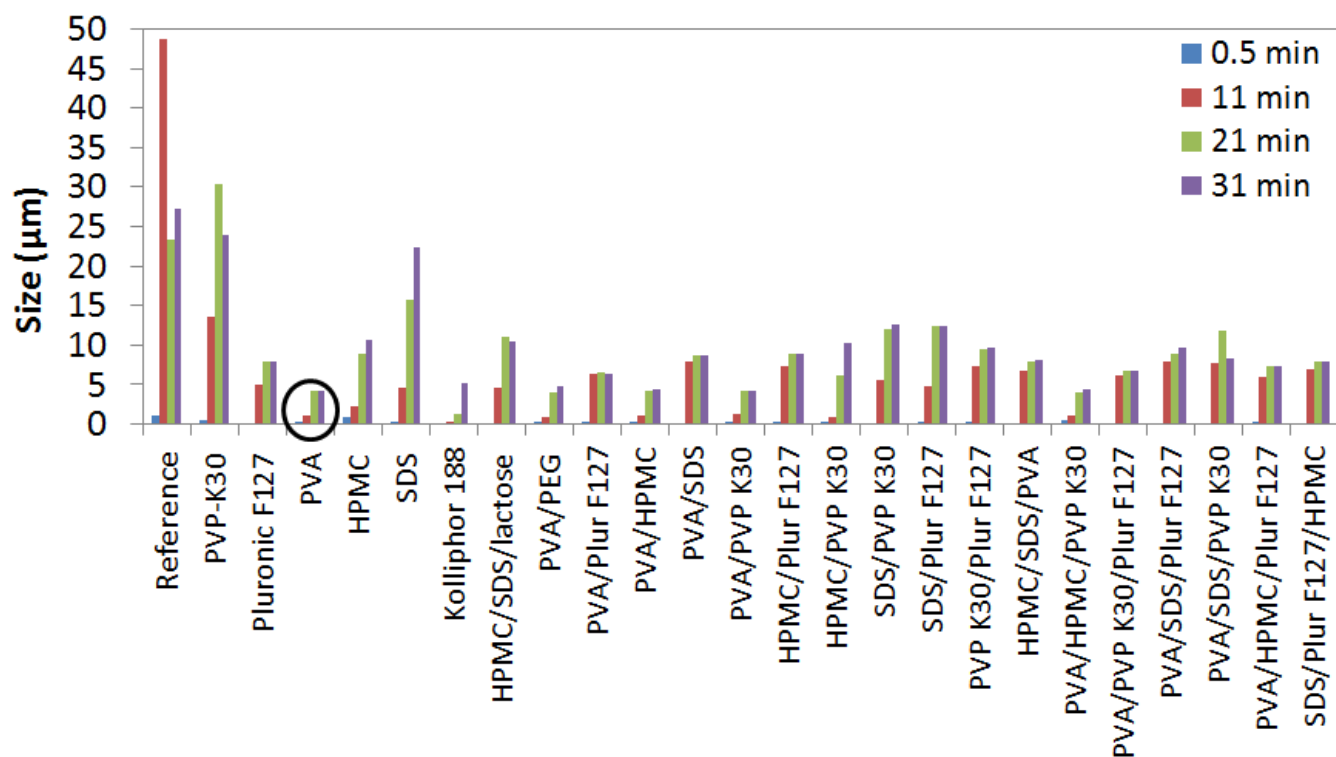
**Figure 2.** Particle size distributions of FF precipitated from varying drug concentrations at an aging time of 0.5 min.

Based on the size results obtained for the reference sample (no additives, Prep A), a drug concentration of 50 mg/mL, an AS/S ratio of 10:1 and an agitation rate of 800 rpm were chosen as the standard process conditions for additive-based precipitation studies.

### **3.2. Effect of additives on the growth of precipitated particles in suspension**

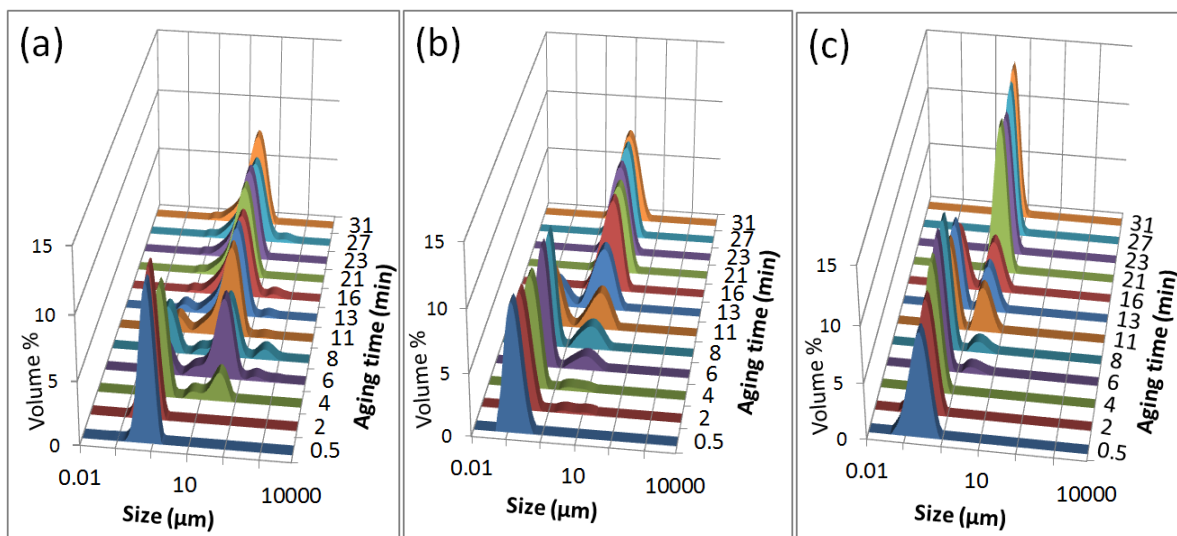
Preparation of submicron particles by precipitation was found to be relatively easy, but stabilization of these particles was more difficult. All additive systems tested provided enhanced stabilization of suspended submicron particles compared to the reference sample, Figure 3. Results pinpointed PVA as the most effective stabilizer both by preserving the particles in the submicron size range for the longest time (~11 min) and by providing long term stabilization for

the 4-5  $\mu\text{m}$  particles which developed by 21 min. Kolliphor 188 also stabilized particles in the submicron range for at least 11 min, but its longer term stabilization ability (beyond 21 min) was poor, with the particles quickly reaching 20  $\mu\text{m}$  (data not shown). No further improvements in stabilization were observed when PVA was used in mixtures with other additives, Figure 3. Additional analysis indicated that PVA with a molecular weight of 9-10 kDa at a concentration of 0.2% w/v provided the optimum stabilization of FF (Figure S2). Increasing the PVA concentration above 0.2% did not improve the stabilization.



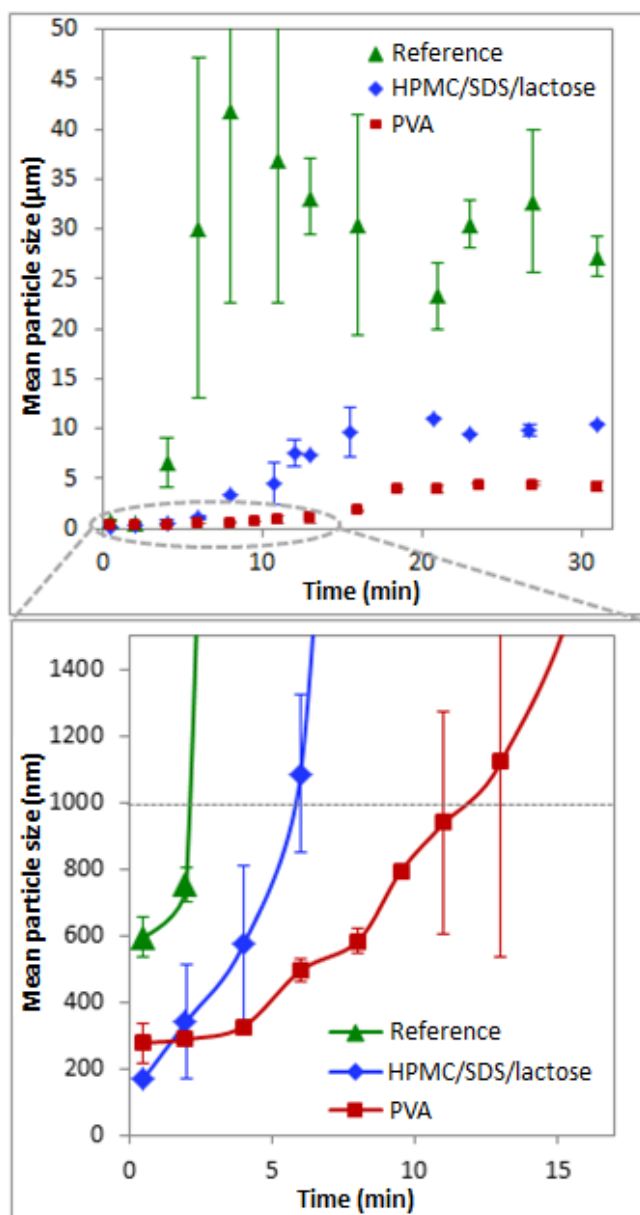
**Figure 3.** Size of precipitated FF as a function of additive system and aging time.

Figure 4 shows the progression of the particle size distributions over time for three antisolvent systems: the reference sample (no additives, Prep A), HPMC/SDS/lactose (as a comparison to results by Hu et al.<sup>11</sup>, Prep B) and PVA (Prep C). The time-resolved graphs in Figure 4 show the time at which the particles grow out of the submicron range.



**Figure 4.** Evolution of the particle size distributions over time for FF precipitated with (a) no additives (reference), (b) HPMC/SDS/lactose and (c) PVA

The mean particle size was determined for each distribution. Figure 5 shows that submicron particles were preserved for 2 min for the reference sample, 6 min when precipitated in HPMC/SDS/lactose and 11 min when precipitated in PVA. In each system, the initial period of slow growth was followed by a period of accelerated growth, before the size plateaued and no further growth occurred, Figure 5.



**Figure 5.** Particle size evolution of FF precipitated with no additives (reference), HPMC/SDS/lactose and PVA

Time-resolved SEM images of oven-dried drops of PVA-precipitated suspensions showed particles with a similar growth rate to the suspended particles, with the size gradually increasing from 0.38  $\mu\text{m}$  to 4.7  $\mu\text{m}$ , at a time scale comparable to that of the suspended particles, Figure 6.

Therefore, particles dried in this way were taken as being representative of the particles in suspension.

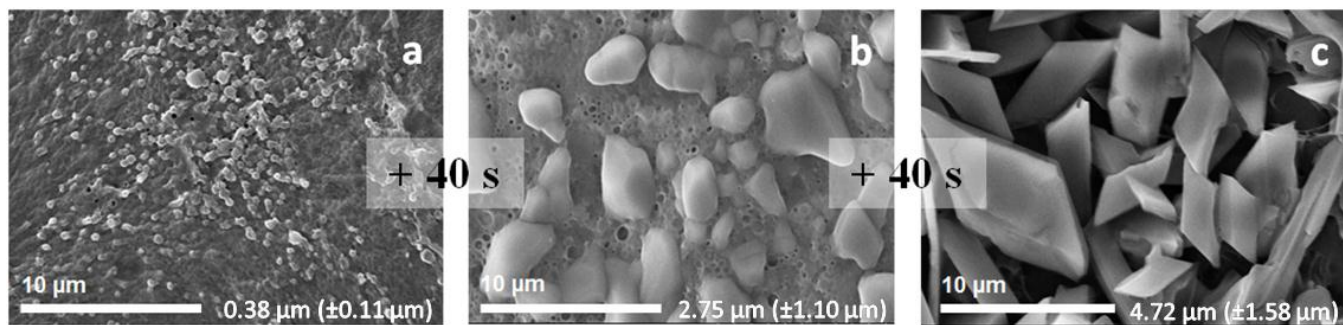


**Figure 6.** SEM images showing the size evolution of oven-dried PVA-precipitated FF particles at 40 second intervals from (a) aging time  $\approx$  12 minutes to (b) to (c). Image (c) represents the final observed particle size and morphology.

The dissolution rate of the suspended submicron PVA-precipitated particles (200-300 nm, 2.55% dissolved/s) was equivalent to that of the commercial formulation (260 nm, 2.45% dissolved/s), Figure 7. The dissolution rate of the larger 4-5 μm particles was lower at 0.55% dissolved/s. Additives were found to have no influence on the solubility of FF in the dissolution media (130 mg/900 ml).

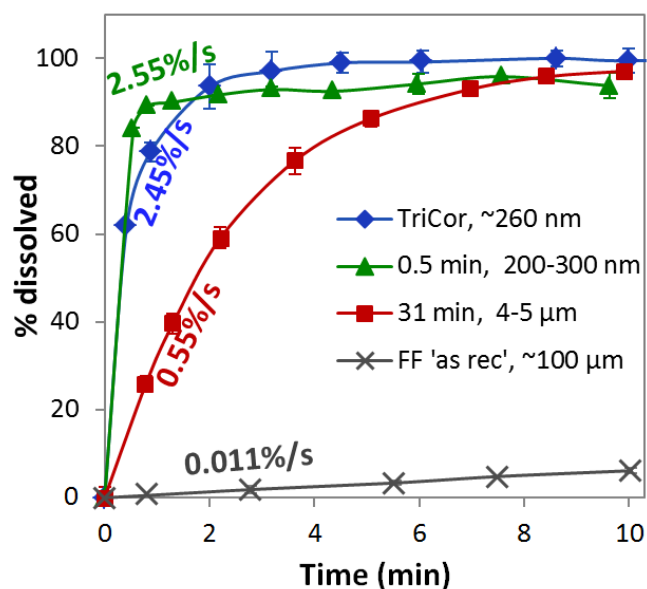


**Figure 7.** Dissolution profiles of commercial and ‘as received’ powder samples and PVA-precipitated suspensions of FF at aging times 0.5 and 31 min.

### 3.3. Effect of freeze-drying on the size and growth pathway

Re-dispersion of freeze-dried particles precipitated from PVA (Prep C) indicated that particles with a pre-dried size of 4-5 μm could maintain their size during drying while submicron particles could not. Particles with a pre-dried size of 200-300 nm grew/agglomerated to 16 μm during drying, as determined by laser diffraction (Figure S3).

SEM images of particles precipitated from all three antisolvent systems (Prep A-C), aged for <2 min, showed limited evidence of submicron particles after freeze-drying. Precipitation from the reference system produced chunky, faceted FF crystals which grew to a mean size of 4.1 μm within 15 minutes (Figure 8a). Precipitation in HPMC/SDS/lactose showed a non-uniform crystal habit over time. Although some sub-micron spheres (0.9 μm) were observed when aged for 2 min, they gradually evolved into flat elongated 4 μm plates with fused tips to form



aggregated structures of approx. 10  $\mu\text{m}$  in length (Figure 8b). Over time, PVA-precipitated FF particles developed from smooth-surfaced but rounded, immature and irregular particles at 0.5 minutes, to roughly-surfaced particles at 11 and 21 minutes, to smooth-surfaced parallelepiped-shaped particles with defined edges at 31 minutes. (Figure 8c, Figure 9).

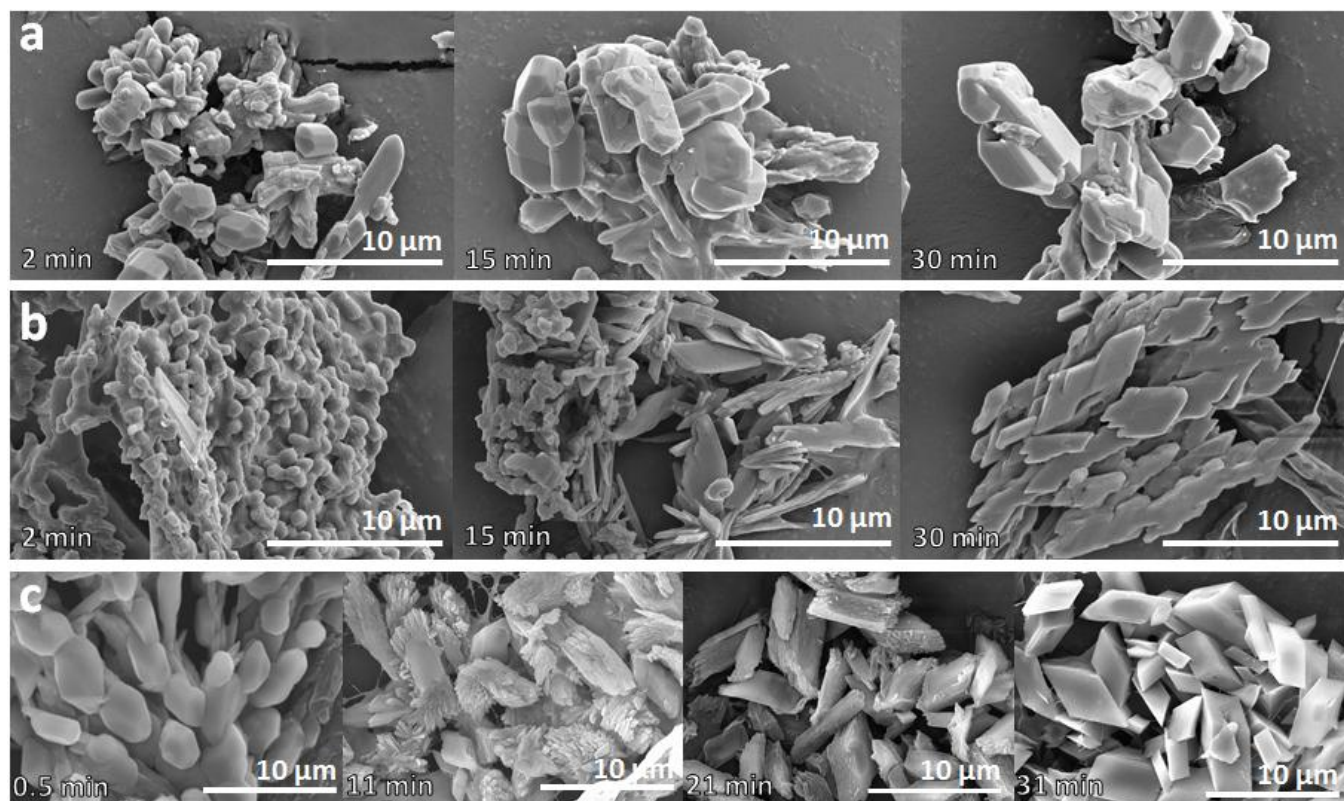


**Figure 8.** Time-resolved SEM images of freeze-dried FF precipitated with (a) no additives (reference) (b) HPMC/SDS/lactose, and (c) PVA.

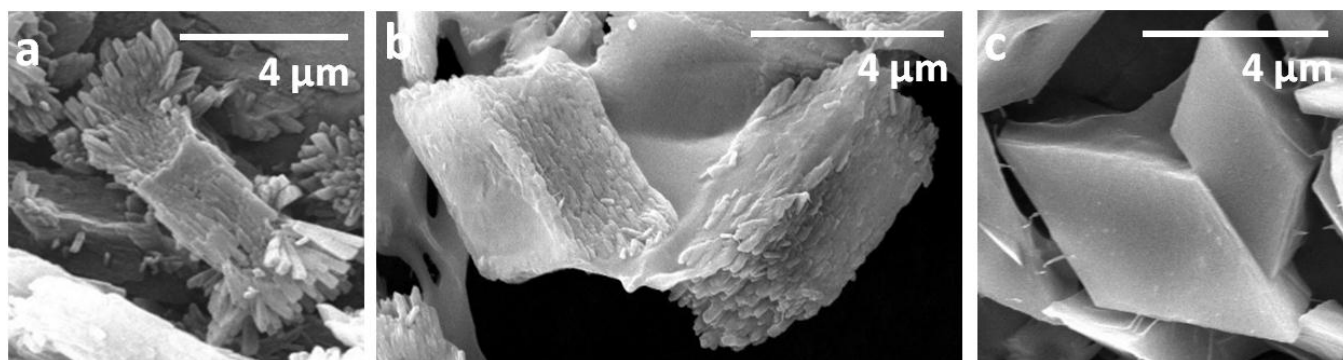


**Figure 9.** Higher magnification SEM images of PVA-precipitated FF at aging times of (a) 11 min, (b) 21 min and (c) 31 min (freeze-dried)

Dissolution testing of freeze-dried samples (Figure 10) showed that dissolution of the reference sample aged for 2 min was higher than that of a sample which was aged for 30 min. The dissolution rate of HPMC/SDS/lactose-precipitated particles, aged for 2 and 30 min were similar. The dissolution rate of PVA-precipitated particles aged for < 2 min was lower than that of particles which were aged for 31 min, Figure 10. The 31 minute PVA-precipitated sample showed the best dissolution rate of all the dried samples (0.45% /s).

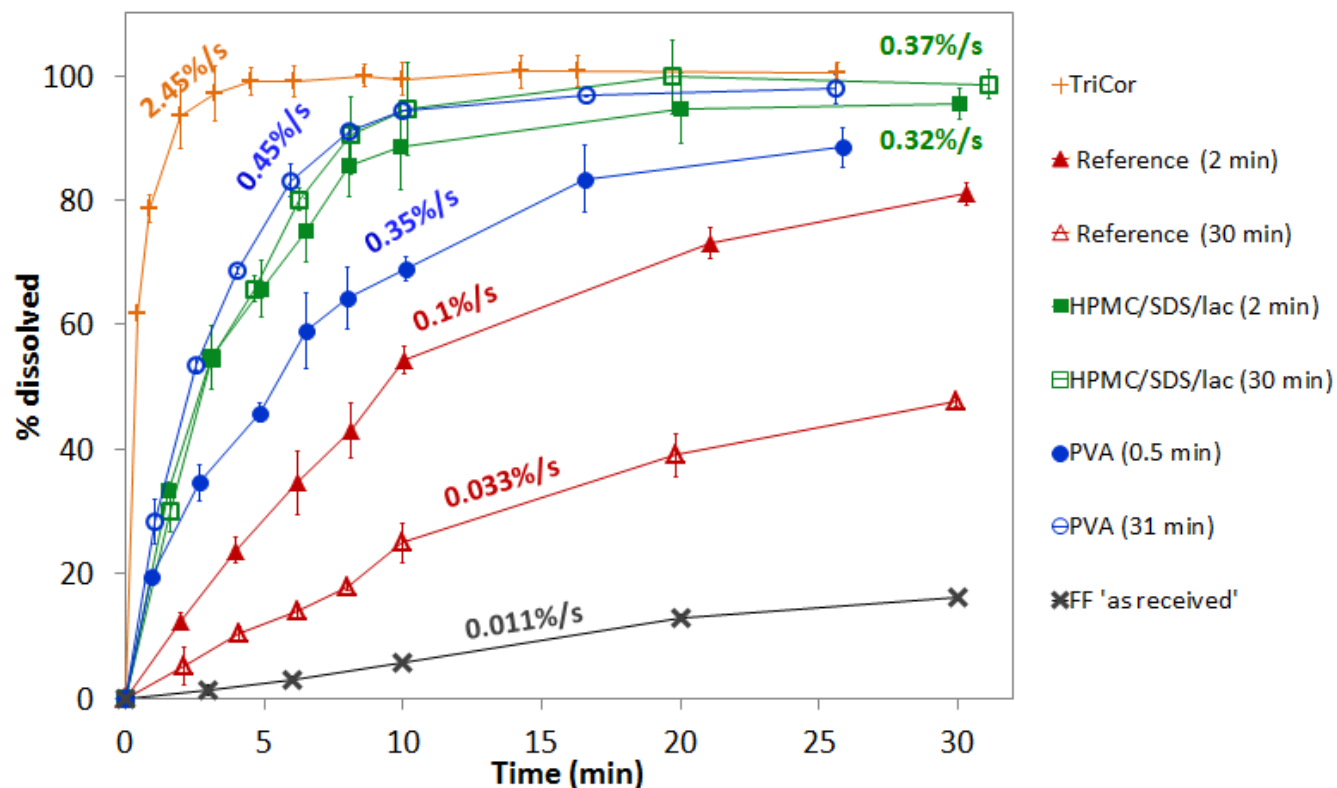


**Figure 10.** Dissolution profiles of freeze-dried FF samples precipitated with no additives (reference), HPMC/SDS/lactose, and PVA, along with the dissolution profiles of the commercial and ‘as received’ samples.

XRD analysis in combination with data from the Cambridge Structural Database showed that all freeze-dried samples precipitated from PVA (Prep C) crystallized in the polymorphic form I (centro-symmetric triclinic space group P-1)<sup>17</sup>. The diffraction patterns are shown in Figure 11.

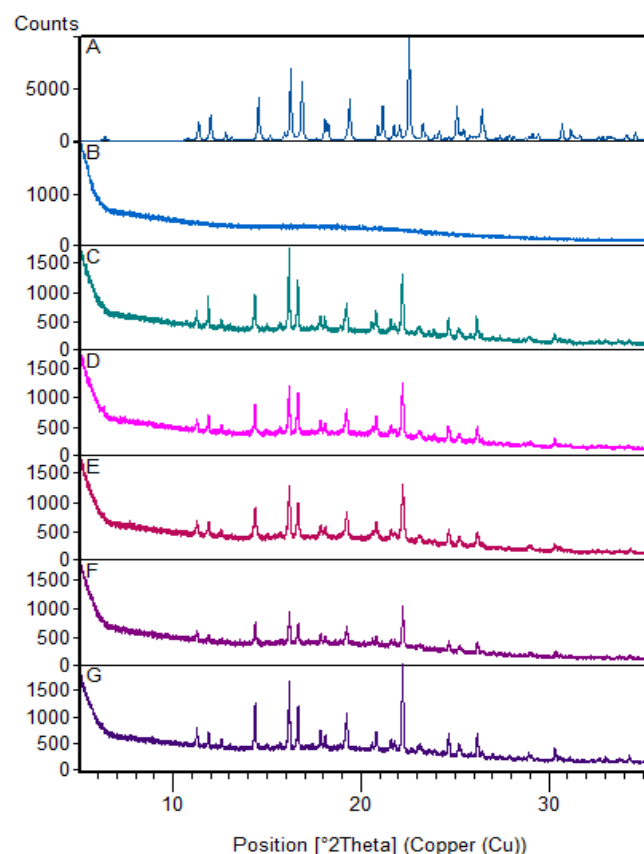


**Figure 11.** X-ray diffraction patterns of (A) theoretical form I (triclinic), (B) blank background, and (C) ‘as received’ FF; and of freeze-dried, PVA-precipitated FF at aging times of (D) 0.5 min, (E) 11 min, (F) 21 min, and (G) 31 min.

Selected area electron diffraction (SAED) patterns of the 11, 21 and 31 minute PVA-precipitated samples (from Figure 9) are shown in Figure 12. Diffraction patterns obtained from the aggregates in the 11 min sample appeared as rings depicting their polycrystalline nature (Figure 12A). Many of the spherical submicron clusters at the tips of the aggregates produced a blurred halo, with no visible discrete diffraction spots, thus showing their amorphous nature (Figure 12B). In contrast, the diffraction patterns obtained from particles in both the 21 min and 31 min samples appeared as discrete, ordered diffraction spots, portraying the particles as single crystals (Figure 12C-D).

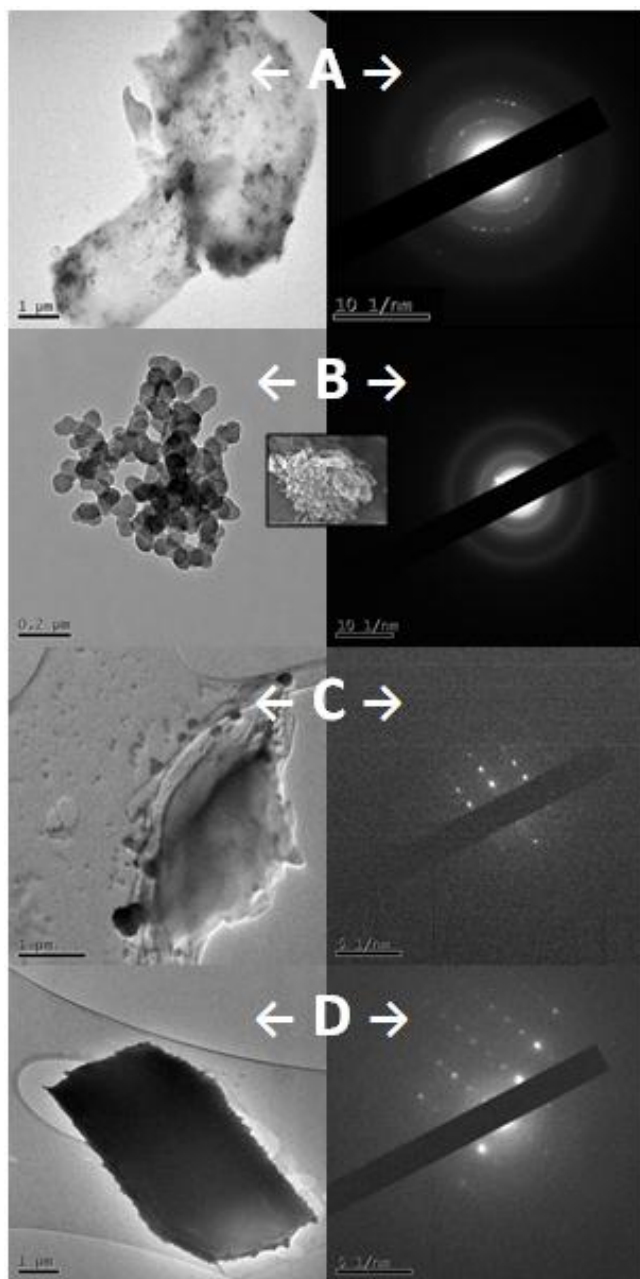


**Figure 12.** TEM micrographs and SAED patterns of freeze-dried, PVA-precipitated FF particles at aging times of (A) 11 min, (B) 11 min (submicron clusters), (C) 21 min, and (D) 31 min

The inner structures of the roughly-surfaced 21 min particles were examined by cutting along the length of the crystals with a focused ion beam. Despite the rough surface on the particle's exterior, the interior was predominantly solid, compact and void of cavities, apart from a

porous/spongy region at each tip, Figure 13. Similar analysis of the 31 min smooth-surfaced particles showed a solid interior with no inner porosity (data not shown).

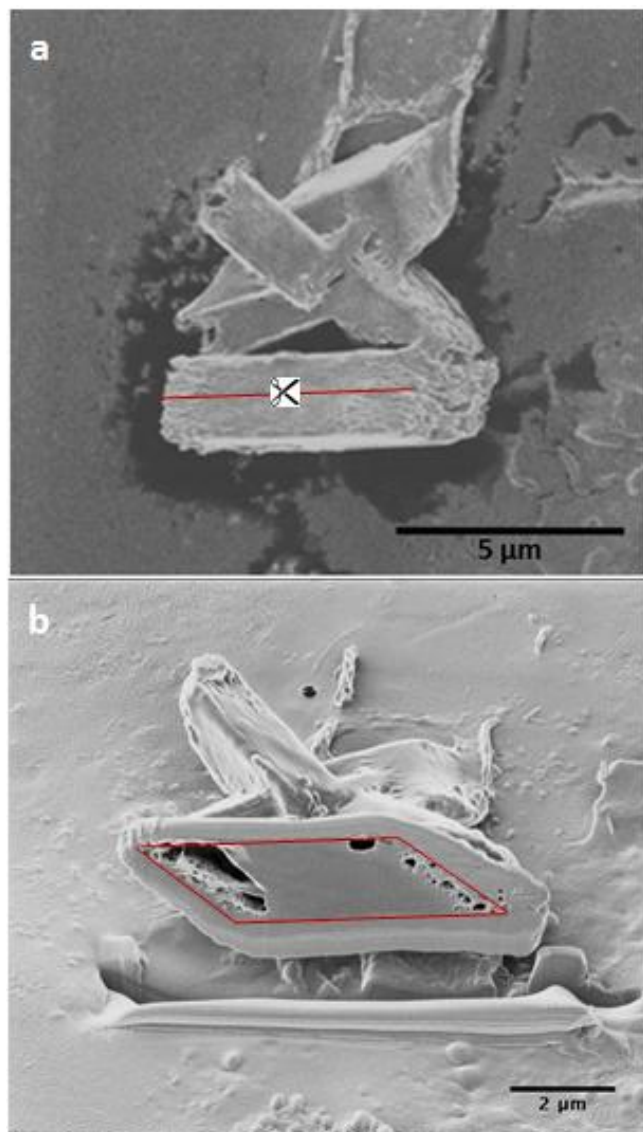


**Figure 13.** Image of a 21 min PVA-precipitated particle (a) before, and (b) after cutting by FIB. The particle in (b) is tilted by 45° and the red line designates the external surface of the original crystal inside a layer of re-deposited material.

#### 4. DISCUSSION

Precipitation is a solid-forming process which is triggered by conditions of high supersaturation. During precipitation, rapid nucleation is followed by particle growth. The supersaturation level controls the nucleation rate which in turn controls the particle size. High supersaturation which is induced by high drug concentration and high AS/S ratio encourages nucleation to dominate over growth, resulting in the formation of smaller particles, as reported previously for many compounds<sup>6,9,18</sup>. The inverse trend between concentration/drug mass and size validates that it is not the growth rate, but the nucleation rate, and ultimately the number of particles that governs the particle size. While these trends were also observed here, it was found that at comparable supersaturation levels, variations in the concentration had a bigger influence on the particle size than variations in the AS/S volume ratio. This result can be explained by differences in the local supersaturation at the point of injection of the drug solution. The drug mass varies with variations in the concentration (at a fixed AS/S ratio). Higher concentration, and thus higher drug mass, induces a steep local supersaturation gradient at the drug solution/antisolvent interface before uniformity is achieved by mixing. The effects of local supersaturation gradients are smaller for changes in the AS/S volume ratio since the added drug mass is constant.

Using optimum antisolvent process parameters, submicron sized particles were successfully produced by antisolvent precipitation. However, due to their high surface energy, additives were required to stabilize the submicron particles in suspension and during isolation. The growth rate of precipitated particles depended on the additive system used. Of the systems tested, PVA provided the most successful stabilization for FF particles in suspension. PVA is an FDA-approved GRAS additive (generally recognized as safe), which has been reported to stabilize particles by coating them with a thick and stable protective layer<sup>19</sup>. This polymer has an

abundance of hydrogen bond donors and no acceptors, while FF has four hydrogen bond acceptors and no donors. This combination gives PVA high potential to hydrogen bond with FF surfaces, thus allowing it superiority over other additives in stabilizing the drug. While many of the other tested additives have functional groups capable of hydrogen bonding (eg. the pluronics, PEG, HPMC, PVP-K30), the presence of hydrogen bond accepting groups in these molecules limits their ability to interact with FF. Molecules with both accepting and donating capabilities can form intramolecular and interchain hydrogen bonds, thus decreasing their drug-polymer interaction potential. The initial stabilization induced by Kolliphor 188 was attributed to its lower molecular weight compared to the other polymers tested, which lessens its steric effects on interacting with the FF molecule. However, the presence of both hydrogen bond accepting and donating groups in this molecule dampens its longer term stabilization abilities. The stabilization efficiency of PVA for the precipitated particles was further improved by selecting the concentration and molecular weight which induced the slowest growth rate. It is likely that these optimum conditions indicate the point at which the surface coverage and coating thickness of the PVA were respectively maximized. PVA enhanced the stability of submicron FF particles compared to that reported previously for this compound under comparable preparation conditions <sup>11</sup>. Unlike other reports which utilize antisolvent precipitation to control the size of FF particles<sup>20-22</sup>, this system was carried out without the addition of ultrasonication, making scale up prospects more feasible. The size and dissolution rate of the suspended PVA-stabilized submicron particles matched those of the milled particles in the commercial formulation, TriCor. To our knowledge this comparison has not been shown in previous reports on precipitated FF <sup>11</sup>,

20, 23, 24



Results from SEM (Figure 8) and dissolution testing (Figure 10) indicated that the precipitated submicron particles were not preserved as individual entities during freeze-drying. For all three antisolvent systems (preparations A-C), the dissolution rates of dried particles (Figure 10) were poorer than those of their suspended equivalents. Dissolution testing of the freeze-dried reference samples (Prep A) showed that an increase in particle size [as observed by SEM, (Figure 8)] resulted in a decrease in dissolution rate (Figure 10). FF precipitated by Prep B showed similar dissolution rates for 0.9  $\mu\text{m}$  spheres at 2 minutes, and 4  $\mu\text{m}$  plates at 30 minutes. The similarity in dissolution rates is attributed to the change in the particle shape from spheres to plates, thus maintaining a relatively constant surface area/volume ratio, Figure 10 and 8b. The poorer dissolution rate of PVA-precipitated FF (Prep C) at 0.5 minutes compared to 31 minutes can only be explained by aggregation and fusion of insufficiently stabilized submicron particles (at 0.5 min) during the destabilizing drying process, Figure 14.]

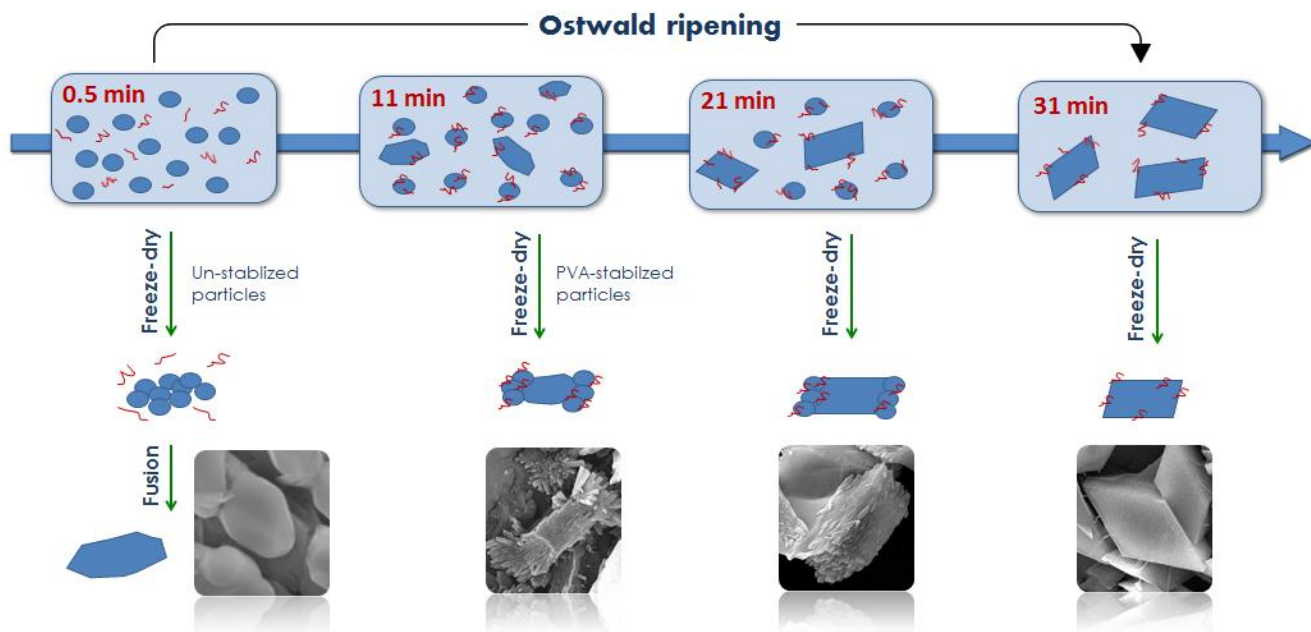


**Figure 14.** Schematic description of the hypothesized growth mechanism of particles in suspension, highlighting the drying-induced morphologies of freeze-dried particles

Visually different growth patterns were detected for PVA-precipitated particles isolated by oven-drying (Figure 6, representative of suspended particles) and those isolated by freeze-drying, Figure 8c, 9. The suspended and oven-dried particles gradually evolved from submicron to small micron size in a manner corresponding to Ostwald ripening. Figure 4 shows the growth of the larger particles in suspension at the expense of the submicron particles. Depletion of the submicron particles prevented further growth in suspension, resulting in a plateaued stable particle size of 4-5  $\mu\text{m}$ . Analysis of freeze-dried particles (Figure 8c) presented a visually different morphological development of particles over time, which appeared inconsistent with the classical Ostwald ripening mechanism. The change in morphologies of the isolated particles from irregular immature crystals at 0.5 min, to aggregated submicron particles at 11 min, to roughly-surfaced and then smooth-surfaced parallelepiped crystals at 21 and 31 min is attributed to the freeze-drying process (Figure 14). While submicron particles existed in suspension at 0.5 min (Figure 5), they were not observed in the corresponding freeze-dried sample (Figure 8c). It is proposed that this short aging time was insufficient for the PVA to bond to, and stabilize the suspended submicron particles. The subsequent drying step caused aggregation, followed by fusion of the un-stabilized 0.5 min particles. At 11 minutes, freeze-drying again forced aggregation of the submicron particles, but the PVA-coating prevented the fusion step from occurring (Figure 14). During the period of accelerated growth between 11 and 21 minutes, submicron and small micron particles coexisted in suspension (Figure 4) but drying forced the submicron particles to surface-attach to the larger particles. By 31 minutes, no submicron particles remained in suspension (Figure 4c). This explains why these particles maintained their smooth surface during drying. Based on time-resolved particle sizing and SEM imaging, it is hypothesized that PVA-precipitated particles grow by Ostwald ripening in suspension followed

by forced aggregation, attachment and/or fusion during the freeze-drying step. It must be clarified that the morphological development of the freeze-dried particles with time is not the result of a continuous growth process, but a knock-on effect from isolation of the growing particles at various time points (Figure 14).

However, SEM analysis alone was insufficient in distinguishing if the visible submicron particles in the 11 and 21 min samples in Figure 8c were truly a surface event or if they extended throughout the entire structure in an assembled fashion (ie. as a mesocrystal). FIB analysis verified that the interior of the 21 minute particles was predominantly solid and free of the cavities which would be associated with particle assembly into mesocrystals. The porous region at the particle tips (consistent for all 21 min particles analyzed) was caused by the visible coating of submicron particles these areas. This porous region was not observed for the smooth-surfaced 31 min particles.

SAED analysis defined the 11 min particles as polycrystals which formed when the submicron particles aggregated during drying. Results showed that particles which were aged for 21 min were single crystals, despite their rough surface. A likely explanation as to how a polycrystalline aggregate would develop into a highly-crystalline single crystal (confirmed by XRD, Figure 11) is through the traditional Ostwald ripening pathway, whereby the inner particle gradually grows at the expense of the remaining submicron particles.

Therefore, despite the appearance of an unusual growth trend for freeze-dried PVA-precipitated FF from time-resolved SEM analysis, results from FIB and SAED indicated that the growth mechanism was no different to that of the suspended particles. The visual differences were found to be related to the drying process. For this reason, examination of the crystal habits alone can be misleading in determining the growth mechanism, leading to frequent

misinterpretation. Results have shown that the effect of the drying process on the system is quite significant and must also be considered.

## **5. CONCLUSION**

Submicron sized FF particles (200-300 nm) were successfully precipitated with an equivalent size and dissolution rate to that of a milled commercial nanoformulation, without the use of ultrasonication. The stability of the particles in the submicron size range was short-lived and additives were required to slow their growth rate. PVA showed the most effective stabilization for FF due to the characteristic hydrogen bonding capabilities of both PVA and FF, compared to the other additives tested. The stabilization of the suspended submicron particles by PVA was only temporary and so immediate isolation was necessary. While freeze-drying proved successful in isolating small-micron sized particles, it was unsuccessful in preserving the pre-dried submicron particles as individual entities during the drying process. The isolation process, which can destabilize high energy submicron particle systems, has yet to be optimized to find the best conditions for preserving the submicron particle in the solid form.

During the course of this work, it was demonstrated that the additives and isolation method used impacted on the final size and shape of the crystals. Both the size and shape were instrumental in influencing the dissolution rate. The growth pathway of FF was probed due to considerable differences in the crystal habits and observed growth patterns of suspended and freeze-dried particles. Despite visual differences, both processes were found to adhere to the traditional growth mechanism of molecular addition by Ostwald ripening. No evidence of orientated attachment or mesocrystal particle assemblies was found. Results indicated that single crystals became coated in a layer of submicron particles during the freeze-drying process. These

results demonstrate the importance of considering the effect of the drying process on the growth mechanism.

## **ASSOCIATED CONTENT**

Electronic supplementary information is available containing figures showing the effects of AS/S volume ratio on the particle size, the effects of PVA concentration and molecular weight on the growth rate of precipitated fenofibrate and the effects of freeze-drying on the re-dispersed particle size. This material is available free of charge via the internet at <http://pubs.acs.org>.

## **AUTHOR INFORMATION**

### **Corresponding Author**

#Email: [Sarah.Hudson@ul.ie](mailto:Sarah.Hudson@ul.ie)

### **Notes**

The authors declare no competing financial interest.

## **ACKNOWLEDGMENT**

We acknowledge the Irish Research Council for funding this project and the Synthesis and Solid State Pharmaceutical Centre and Science Foundation Ireland for their additional support. We also acknowledge the Program for Research in Third-Level Institutions (PRTLII) Cycle 5 and the European Regional Development Fund for their role in funding certain elements of this project.

## **REFERENCES**

(1) Merisko-Liversidge, E.; Liversidge, G. G.; Cooper, E. R., Nanosizing: a formulation approach for poorly-water-soluble compounds. *Eur. J. Pharm. Sci.* **2003**, 18, 113-120.

- (2) Rawat, N.; Kumar, M. S.; Mahadevan, N., Solubility: Particle Size Reduction is a Promising Approach to Improve the Bioavailability of Lipophilic Drugs. *Int. J. Rec. Adv. Pharm. Res.* **2011**, 8-18.
- (3) Kesisoglou, F.; Panmai, S.; Wu, Y., Nanosizing — Oral formulation development and biopharmaceutical evaluation. *Adv. Drug Delivery Rev.* **2007**, 59, 631-644.
- (4) Duncan, R.; Gaspar, R., Nanomedicine(s) under the Microscope. *Mol. Pharmaceutics* **2011**.
- (5) Parikh, D. M., *Handbook of Pharmaceutical Granulation Technology*. ed.; Marcel Dekker: New York, 1997; Vol. 81.
- (6) Wang, Z.; Chen, J.-F.; Le, Y.; Shen, Z.-G.; Yun, J., Preparation of Ultrafine Beclomethasone Dipropionate Drug Powder by Antisolvent Precipitation. *Ind. Eng. Chem. Res.* **2007**, 46, 4839-4845.
- (7) Bansal, S., Nanocrystals: Current Strategies and Trends. *Int. J. Res. Pharm. Biomed. Sci.* **2012**, 3, 406-419.
- (8) Yaeger, S. A., Innovative Milling & Micronization Techniques for the Pharmaceutical Industry. In ed.; **2008**.
- (9) Park, M.-W.; Yeo, S.-D., Antisolvent crystallization of carbamazepine from organic solutions. *Chem. Eng. Res. Des.* **2012**.
- (10) Paulino, A. S.; Rauber, G.; Campos, C. E.; Mauricio, M. H.; de Avillez, R. R.; Capobianco, G.; Cardoso, S. G.; Cuffini, S. L., Dissolution enhancement of Deflazacort using

hollow crystals prepared by antisolvent crystallization process. *Eur. J. Pharm. Sci.* **2013**, 49, 294-301.

(11) Hu, J.; Ng, W. K.; Dong, Y.; Shen, S.; Tan, R. B. H., Continuous and scalable process for water-redispersible nanoformulation of poorly aqueous soluble APIs by antisolvent precipitation and spray-drying. *Int. J. Pharm.* **2011**, 404, 198-204.

(12) Khan, S.; Matas, M. d.; Zhang, J.; Anwar, J., Nanocrystal Preparation: Low-Energy Precipitation Method Revisited. *Cryst. Growth Des.* **2013**, 13, 2766-2777.

(13) Song, R.-Q.; Colfen, H., Mesocrystals-Ordered Nanoparticle Superstructures. *Adv. Mater.* **2010**, 22, 1301-1330.

(14) Thorat, A. A.; Dalvi, S. V., Particle formation pathways and polymorphism of curcumin induced by ultrasound and additives during liquid antisolvent precipitation. *CrystEngComm* **2014**, 16, 11102-11114.

(15) Al-Dhalli, S. Preparation and Evaluation of Fenofibrate-Gelucire 44/14 Solid Dispersions. 2007.

(16) Junghanns, J. U.; Muller, R. H., Nanocrystal technology, drug delivery and clinical applications. *Int. J. Nanomed.* **2008**, 3, 295-309.

(17) Henry, R. F.; Zhang, G. Z.; Gao, Y.; Buckner, I. S., Fenofibrate. *Acta Crystallogr., Sect. E* **2003**, 59, 0699 - 0700.

(18) Lonare, A.; Patel, S. R., Antisolvent Crystallization of Poorly Water Soluble Drugs. *Int J Chem Eng Appl.* **2013**, 4.

- (19) Abdelwahed, W.; Degobert, G.; Stainmesse, S.; Fessi, H., Freeze-drying of nanoparticles: Formulation, process and storage considerations. *Adv. Drug Delivery Rev.* **2006**, 58, 1688-1713.
- (20) Zhang, H.; Meng, Y.; Wang, X.; Dai, W.; Wang, X.; Zhang, Q., Pharmaceutical and pharmacokinetic characteristics of different types of fenofibrate nanocrystals prepared by different bottom-up approaches. *Drug delivery* **2014**, 21, 588-594.
- (21) Meng, X.; Chen, Y.; Chowdhury, S. R.; Yang, D.; Mitra, S., Stabilizing dispersions of hydrophobic drug molecules using cellulose ethers during anti-solvent synthesis of micro-particulates. *Colloids Surf., B* **2009**, 70, 7-14.
- (22) Beck, C.; Dalvi, S. V.; Dave, R. N., Controlled liquid antisolvent precipitation using a rapid mixing device. *Chem. Eng. Sci.* **2010**, 65, 5669-5675.
- (23) Dong, Y.; Ng, W. K.; Hu, J.; Shen, S.; Tan, R. B. H., Clay as a matrix former for spray drying of drug nanosuspensions. *Int. J. Pharm.* **2014**, 465, 83-89.
- (24) Dong, Y.; Ng, W. K.; Hu, J.; Shen, S.; Tan, R. B. H., Continuous production of redispersible and rapidly-dissolved fenofibrate nanoformulation by combination of microfluidics and spray drying. *Powder Technol.* **2014**, 268, 424-428.

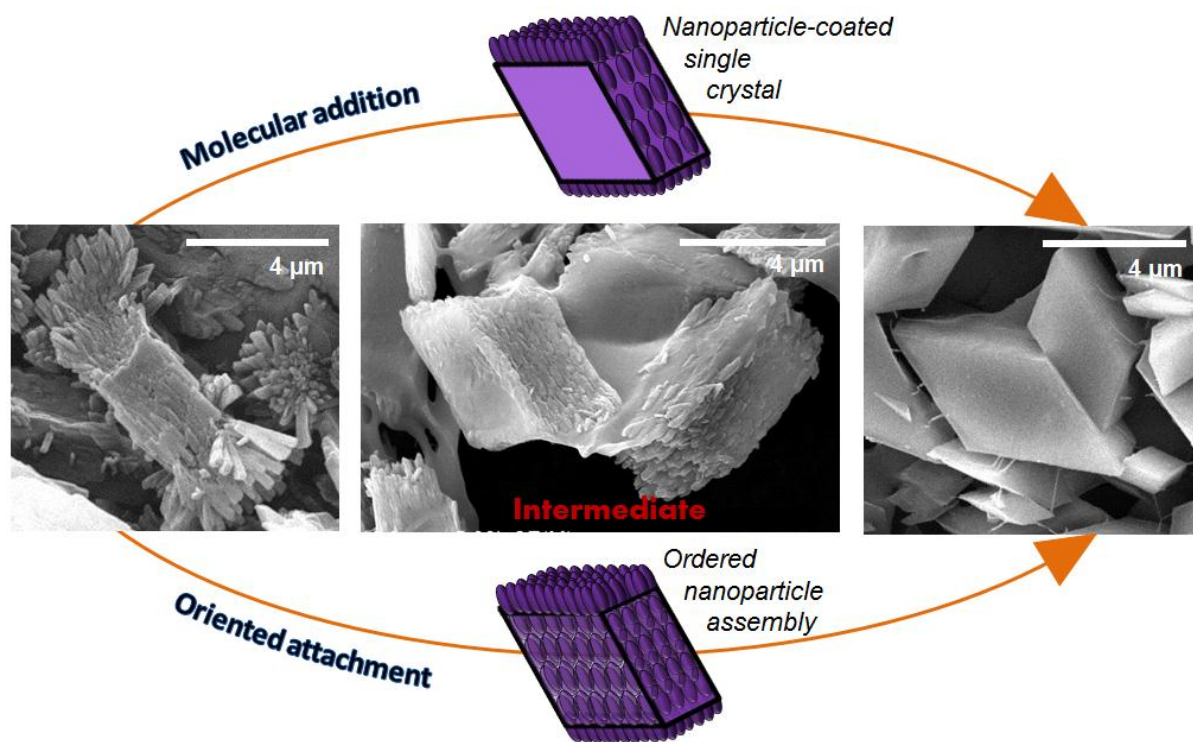


## For Table of Contents Use Only

# An Investigation of the Particle Growth of Fenofibrate following Antisolvent Precipitation and Freeze-drying

*Teresa B. Tierney, Yina Guo, Sergey Beloshapkin, Åke C. Rasmuson, and Sarah P.*

*Hudson*



Following antisolvent precipitation and freeze-drying of fenofibrate, roughly-surfaced intermediate particles were observed. Both molecular addition and orientated attachment-based growth mechanisms were considered in an attempt to explain the particle roughness. Results showed that suspended particles grew by molecular addition and that the observed roughness in the dried particles was a result of the freeze-drying process.